The Astrophysical Journal, 588:L53–L56, 2003 May 1

RAPID ACCELERATION OF A CORONAL MASS EJECTION IN THE LOW CORONA AND IMPLICATIONS FOR PROPAGATION

Peter T. Gallagher[1], Gareth R. Lawrence,[2] and Brian R. Dennis
Laboratory for Astronomy and Solar Physics, NASA Goddard Space Flight Center, Greenbelt, MD 20771
Received 2002 December 19; accepted 2003 March 25; published 2003 April 4

ABSTRACT

A high-velocity coronal mass ejection (CME) associated with the 2002 April 21 X1.5 flare is studied using a unique set of observations from the *Transition Region and Coronal Explorer* (*TRACE*), the Ultraviolet Coronagraph Spectrometer (UVCS), and the Large Angle and Spectroscopic Coronagraph (LASCO). The event is first observed as a rapid rise in *GOES* X-rays, followed by two simultaneous brightenings that appear to be connected by an ascending looplike feature. While expanding, the appearance of the feature remains remarkably constant as it passes through the *TRACE* 195 Å passband and LASCO fields of view, allowing its height-time behavior to be accurately determined. The acceleration is consistent with an exponential rise with an *e*-folding time of ~138 s and peaks at ~1500 m s^{-2} when the leading edge is at ~1.7 $R_\odot$ from Sun center. The acceleration subsequently falls off with an *e*-folding time of over 1000 s. At distances beyond ~3.4 $R_\odot$, the height-time profile is approximately linear with a constant velocity of ~2500 km s^{-1}. These results are briefly discussed in light of recent kinematic models of CMEs.

Subject headings: Sun: corona — Sun: coronal mass ejections (CMEs) — Sun: flares

1. INTRODUCTION

Coronal mass ejections (CMEs) are among the largest energy releases in the solar system and can directly affect space weather in the near-Earth environment. Although of such practical importance, the physical mechanisms responsible for CME initiation, acceleration, and propagation remain unclear, despite their having been observed and studied for upward of 20 years (Crooker, Joselyn, & Feynman 1997; Song, Singer, & Siscoe 2001).

It is well known that CMEs are associated with both filament eruptions and solar flares (Zhang et al. 2002; Moon et al. 2002), but the driver mechanism remains elusive. Several possible drivers are described by Krall et al. (2000, 2001), within the context of the flux rope model of Chen (1989, 1996). These include flux injection, footpoint twisting, magnetic energy release, and hot plasma injection. An alternative to this flux rope model is the so-called magnetic break-out model of Antiochos, DeVore, & Klimchuk (1999), in which the CME eruption is triggered by reconnection between the overlying unsheared field and a neighboring flux system. Another possibility is the Forbes & Priest (1995) model, in which a converging flow toward the neutral line results in reconnection beneath the flux rope. These, together with other directly driven and storage-release CME initiation models, are discussed in Klimchuk (2001).

Following initiation, the CME plasma and associated field are accelerated away from the solar surface, with velocities of over ~1000 km s^{-1} within $\lesssim 3\ R_\odot$ (St. Cyr et al. 1999; Zhang et al. 2001; Alexander, Metcalf, & Nitta 2002). For the event discussed here, the heights and times of the first two data points measured above 3 $R_\odot$ by the Large Angle and Spectroscopic Coronagraph (LASCO; Brueckner et al. 1995) imply a mean transit speed of 2400 km s^{-1} between them. Such high velocities are not inferred from low coronal data, nor is even the greatest acceleration inferred from LASCO data (107 m s^{-2}; S. Yashiro et al. 2003, in preparation) sufficient to accelerate a CME constantly to such a speed between 1 and 3 $R_\odot$. Once accelerated, most CMEs assume a near-linear height-time evolution as plasma density, magnetic field, and gravity drop off (Chen et al. 2000); this phase becomes important for heights greater than ~5 $R_\odot$ and can be characterized by a constant velocity or ballistic motion.

In this Letter, we present and analyze data from an event unusual in two regards: its speed and coverage. Its mean linear speed through LASCO is within the fastest 1% of CME speeds inferred from LASCO data (S. Yashiro et al. 2003, in preparation). Also, to complement the LASCO observations, in this case we are able use the *Transition Region and Coronal Explorer* (*TRACE*; Handy et al. 1999) images and the *Solar and Heliospheric Observatory*'s Ultraviolet Coronagraph Spectrometer (UVCS; Kohl et al. 1995). *TRACE*'s cadence and field of view allow CME identification and tracking through the low corona, while UVCS provides data from a critical region that cannot often be incorporated into such studies. This leads to strict constraints on the height-time profile and hence on the derived acceleration profile. In § 2, we describe the observations and data processing, while the curve-fitting techniques used to characterize the CME evolution are described in § 3. Our discussion and conclusions are then presented in § 4, with particular attention to the implications of our results for the various CME initiation and propagation models.

2. OBSERVATIONS AND DATA ANALYSIS

The 2002 April 21 X1.5 flare occurred in NOAA 9906 from approximately 00:43 UT as the region rotated off the southwest limb. In part because this $\beta\gamma\delta$ region was the Max Millennium[3] target for this period, this was an exceptionally well-observed event.

The *TRACE* observations were taken during a standard 195 Å bandpass observing campaign that provides 20 s cadence and an image scale of 0.″5 $pixel^{-1}$. Standard image corrections were first applied before pointing offsets were accounted for using the methods described in Gallagher et al. (2002).

A sample of three *TRACE* difference images is given in the

[1] L-3 Communications EER Systems, Inc., 3750 Centerview Drive, Chantilly, VA 20151.
[2] Center for Solar Physics and Space Weather, Catholic University of America, 620 Michigan Avenue, Washington, DC 20064.
[3] See http://solar.physics.montana.edu/max_millennium.

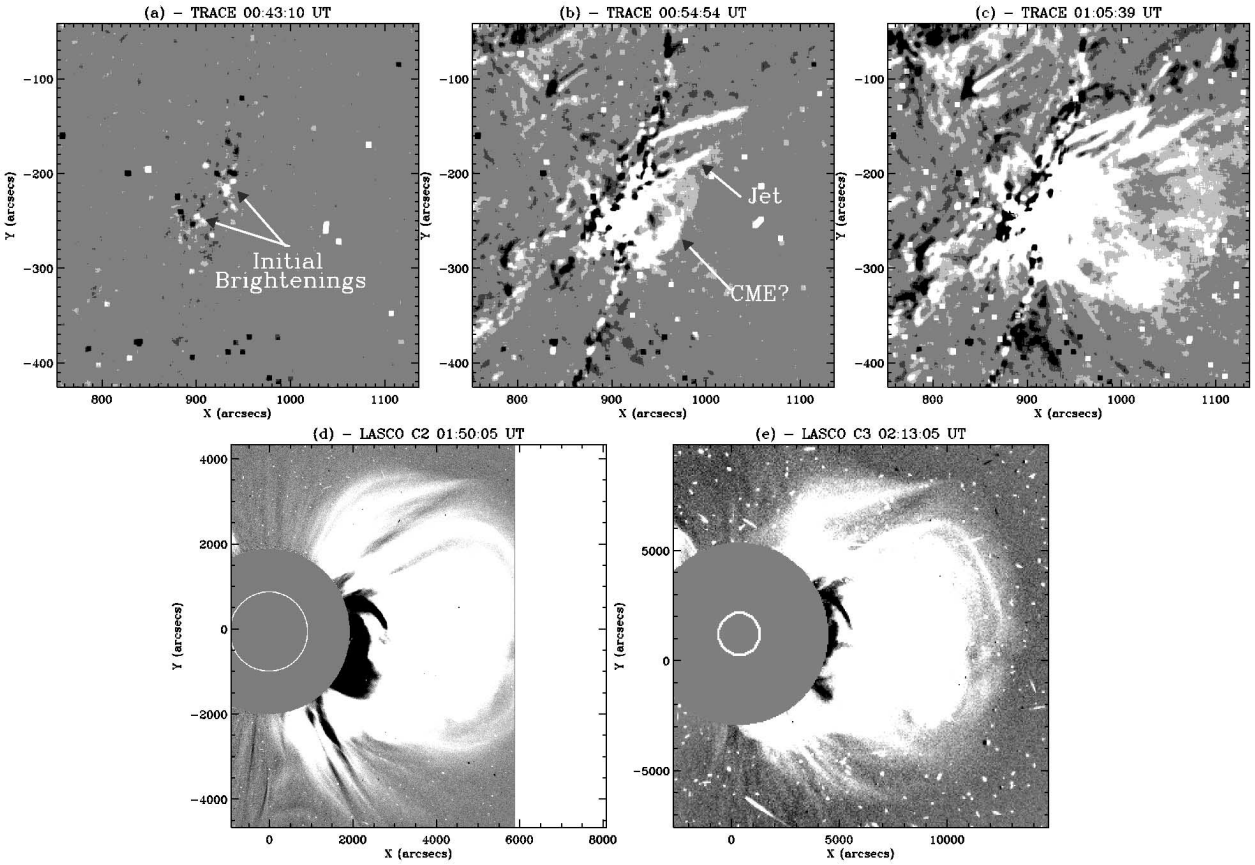

FIG. 1.—*Top panels: TRACE* 195 Å difference images created by subtracting each image from a frame taken at 00:42:30 UT. *Bottom panels:* LASCO C2 and C3 images showing the similar morphology of the eruption as it propagates away from the solar surface.

top row of Figure 1. Figure 1*a* shows a pair of brightenings that first become apparent at ~00:43:10 UT, just as the *GOES-10* soft X-ray flux begins to rise (see Fig. 3*d*). This is then followed at 00:44:53 UT by a linear jetlike feature emerging from close to the westernmost footpoint (Wang et al. 2002). Some 4 minutes later, at 00:48:54 UT, a looplike feature becomes apparent and begins its ascent. The loop is clearest in the 00:54:54–00:42:30 UT difference image in Figure 1*b*. Figure 1*c* later shows a difference image in which the expanded loop is visible to an altitude of ~1.2 $R_\odot$. A height-time profile was extracted from the *TRACE* difference movie using a simple point-and-click methodology to track the feature's apex height above the limb. This method is expected to provide heights with an accuracy of better than ± 5 pixels. The resulting data points and error bars are plotted in Figures 2 and 3.

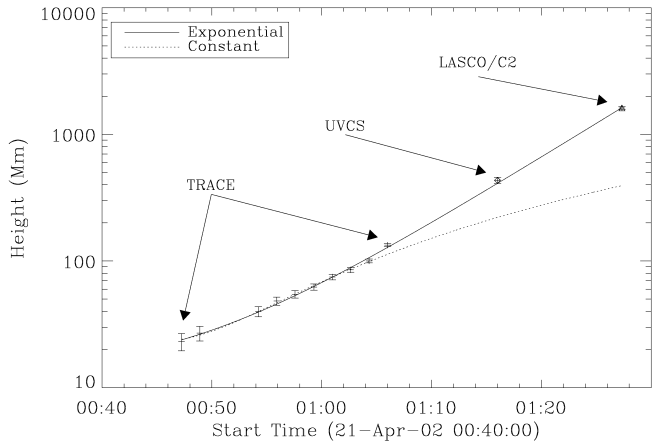

FIG. 2.—Height-time evolution of the 2002 April 21 CME from *TRACE*, UVCS, and LASCO C2. The data are shown with ± 5 pixel error bars. Also given are best fits of eqs. (1) and (2) to the data.

The UVCS instrument has two UV channels capable of measuring UV spectra at 1.4–10 $R_\odot$. On 2002 April 21, the UVCS slit was located directly above NOAA 9906, at a position angle of 262° and an altitude of 1.63 $R_\odot$. At ~01:00 UT, a gradual dimming was observed in O VI and Si XII, followed by a brightening in Fe XVIII and Si XII at ~01:15 UT. This is assumed to be from hot CME material first seen in the *TRACE* 195 Å images. The UVCS point, plotted in Figures 2 and 3, represents a critical datum bridging the *TRACE* and LASCO C2 fields.

LASCO first observed the CME in C2 images at 01:27 UT and in C3 images at 01:42 UT. Figures 1*d* and 1*e* give two difference images from LASCO C2 and C3 taken at 01:50 and 02:13 UT, respectively. Leading-edge (LE) heights above the limb and associated times are shown in Figure 3*a*. Since all the low coronal data discussed above show the eruption to have occurred within a few degrees of the west limb, it is assumed that any projection effects on these heights and any quantities derived from them will be minimal. Although the CME has white-light emission around all 360° of the occulting disk in both C2 and C3 images, that due to the CME is restricted to the 93° between position angles of 213° and 303°. From Figure 1, it is clear that the LE is discernible from *TRACE*, through LASCO C2 and C3.

3. CURVE FITTING

The apparent height of the LE for ~00:47–01:28 UT is plotted in Figure 2 using data from *TRACE*, UVCS, and LASCO

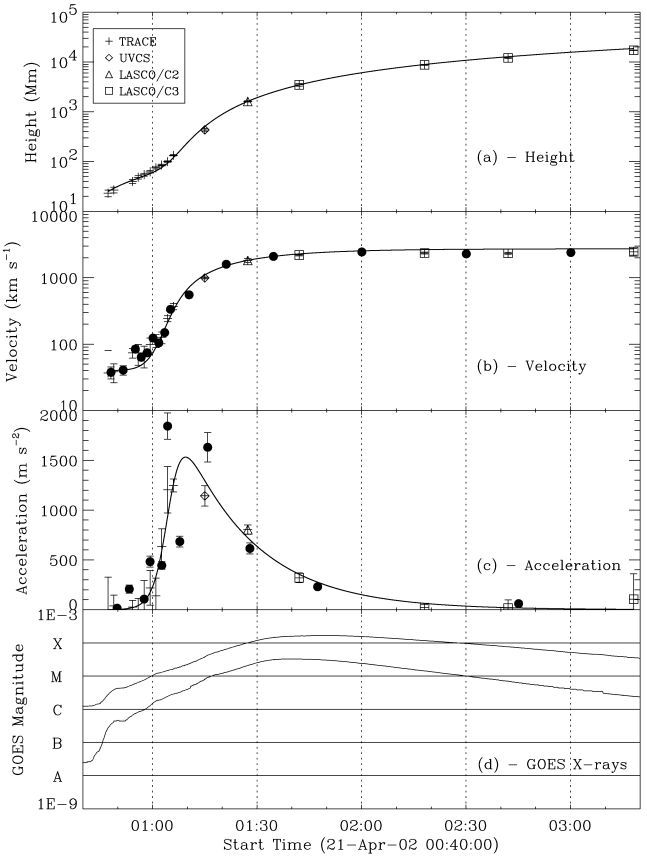

FIG. 3.—(*a*) The height-time profile for ~00:47–03:20 UT; (*b*) and (*c*) give the velocity and acceleration profiles, obtained by taking the first and second numerical derivatives, respectively. The first-difference values are given as filled circles, while the three-point difference values are given using the same symbol scheme as (*a*). The solid line gives the best fit to the data using eq. (4). (*d*) The *GOES-10* soft X-ray flux for the corresponding time period.

C2. Error bars on the data points represent our best estimates of the uncertainties based on the difficulty in identifying the CME LE in each image.

Of particular interest is the acceleration time history, since this is related directly to the driving forces involved. This can be readily derived from the height-time profile by double differentiation. First, the CME velocity points plotted in Figure 3*b* were calculated from the altitude measurements using both first-difference and three-point numerical differentiation. It can be seen that the velocity initially rises rapidly before reaching a constant value of ~2500 km s^{-1} after ~01:30 UT. The acceleration points plotted in Figure 3*c* were calculated from the velocity points in a similar way. They show a rapid increase in acceleration up to a peak at ~01:10 UT, with a falloff to near zero by ~02:30 UT.

To quantify the height-time profile, we consider three acceleration models. The first assumes constant acceleration, the second a simple exponential rise, while the third includes an exponential rise followed by an exponential decay. Each acceleration model can be numerically integrated to obtain the height-time profile as follows:

$$h(t) = h_0 + v_0 t + \int_0^t \int_0^t a(t)dt\,dt, \qquad (1)$$

where t is the time after initiation (taken to be ~00:47 UT), h_0 and v_0 are the initial height and velocity, respectively, and $a(t)$ is the acceleration.

Following Alexander et al. (2002), the simple case of constant acceleration that might apply early in the time history is considered. This results in a height-time profile of the following form:

$$h(t) = h_0 + v_0 t + \tfrac{1}{2} a t^2. \qquad (2)$$

The best-fit to the data points up to 01:06 UT gives $h_0 = 24 \pm 3$ Mm, $v_0 = 13 \pm 13$ km s^{-1}, and $a = 117 \pm 24$ m s^{-2}. As can be seen from Figure 2, the fit does not well represent the UVCS and LASCO C2 data points but is acceptable for heights within the *TRACE* field of view.

An exponentially varying acceleration of the form $a_0 \exp(t/\tau)$ results in the following height-time relationship:

$$h(t) = h_0 + v_0 t + a_0 \tau^2 \exp(t/\tau). \qquad (3)$$

As seen in Figure 2, this function, with $h_0 = 12 \pm 3$ Mm, $v_0 = 0 \pm 13$ km s^{-1}, $a_0 = 48 \pm 2$ m s^{-2}, and $\tau = 486 \pm 8$ s, provides an acceptable fit to the *TRACE*, UVCS, and LASCO C2 points.

The acceleration time data in Figure 3*b* suggests an exponential rise, followed by an exponential decay. A function that shows this behavior is

$$a(t) = \left[\frac{1}{a_r \exp(t/\tau_r)} + \frac{1}{a_d \exp(-t/\tau_d)}\right]^{-1}, \qquad (4)$$

where a_r and a_d are the initial accelerations and τ_r and τ_d give the *e*-folding times for the rise and decay phases. A best fit to the height, velocity, and acceleration data was obtained with $h_0 = 25 \pm 2$ Mm, $v_0 = 40 \pm 4$ km s^{-1}, $a_r = 1 \pm 1$ m s^{-2}, $\tau_r = 138 \pm 26$ s, $a_d = 4950 \pm 926$ m s^{-2}, and $\tau_d = 1249 \pm 122$ s and is shown in Figure 3.

It is interesting to note that the start of the acceleration at ~00:47 UT coincides with the start of the hard X-ray emission at energies above ~25 keV as measured with the *Ramaty High Energy Solar Spectroscopic Imager* (*RHESSI*; Gallagher et al. 2002). Furthermore, the maximum acceleration occurs at about the same time as the peak flux in ≥25 keV emission. This suggests a possible connection between the nonthermal flare energy release and the CME driving force. Another interesting temporal coincidence is the end of the CME acceleration (~02:50 UT) and the change in the upward velocity of the soft X-ray–emitting region from ~10 to ~2 km s^{-1} (at approximately 03:00 UT), also measured with *RHESSI* (Gallagher et al. 2002).

4. DISCUSSION AND CONCLUSIONS

The acceleration and propagation of the (X1.5 related) fast CME of 2002 April 21 has been analyzed using a combination of data from *TRACE*, UVCS, and LASCO. A looplike feature is first observed in *TRACE* 195 Å difference images at 00:48:54 UT, or approximately 5 minutes after a pair of simultaneous brightenings are observed. Following this, the CME passes rapidly through the *TRACE*, UVCS, and LASCO fields of view. The CME initially accelerates to a velocity of ~900 km s^{-1} within approximately 20 minutes, with acceleration peaking at ~1500 m s^{-2} at ~1.7 $R_\odot$ (at ~01:10 UT). Following this peak, the acceleration then decreases with an *e*-folding time of 1249 ± 122 s. At heights beyond ~3.4 $R_\odot$, the height-time profile is well approximated with a con-

stant velocity of ~2500 km s^{-1}. These values are similar to those derived from a CME-related X-ray feature reported by Alexander et al. (2002) using *Yohkoh*/Soft X-ray Telescope and LASCO data.

The findings of this Letter support the flare-associated CME scenario of Zhang et al. (2001), who propose a three-component kinematic evolution consisting of an initiation phase, a rapid acceleration phase, and a propagation phase. The initiation phase is characterized by a slow rise with speeds of $\lesssim$80 km s^{-1}, which adequately accounts for the *TRACE* data taken before ~00:50 UT. The acceleration phase typically lasts for the duration of the soft X-ray rise phase; the 2002 April 21 CME is accelerated for about 50–60 minutes, while the *GOES* X-ray flux reaches a peak on a similar timescale. The propagation phase proposed by Zhang et al. (2001) can then be characterized by a constant or slowly decreasing speed; the CME studied in this Letter reaches a constant velocity within about 1.5 hr of initiation.

As the positions and start times of the CME and flare are well correlated, it is possible that CME initiation could have resulted from either a thermal blast or a hot plasma injection (Krall et al. 2000). On the other hand, the early stages of the flare could be associated with reconnection of overlying magnetic field lines above the region's neutral line. We also note from *TRACE* and EUV Imaging Telescope (EIT) 195 Å images that an arcade of bright post-eruption loops first became visible at ~01:31 UT. Considering that the CME is first observed at ~00:48 UT, models that require near-simultaneous arcade formation and CME acceleration may be appropriate, as it would take approximately 30 minutes for flare/CME loops to cool into the *TRACE* and EIT 195 Å passbands.

Although we have been able to characterize the kinematic evolution of a CME from close to the solar surface to some 26 $R_\odot$, the basic physical mechanisms responsible for initiating and accelerating the CME remain unclear. For predicting accurate CME arrival times at 1 AU and other future efforts in space weather and solar activity forecasting, a deeper understanding of these problems must be obtained.

We are grateful to the anonymous referee for helpful comments. The *Solar and Heliospheric Observatory* is a project of international collaboration between ESA and NASA. The authors wish to acknowledge the support of the LASCO, UVCS, and *TRACE* teams during this work.

REFERENCES

Alexander, D., Metcalf, T. R., & Nitta, N. 2002, Geophys. Res. Lett., 29(10), 1403
Antiochos, S. K., DeVore, C. R., & Klimchuk, J. A. 1999, ApJ, 510, 485
Brueckner, G. E., et al. 1995, Sol. Phys., 162, 357
Chen, J. 1989, ApJ, 338, 453
———. 1996, J. Geophys. Res., 101, 27,499
Chen, J., et al. 2000, ApJ, 533, 481
Crooker, N., Joselyn, J. A., & Feynman, J., eds. 1997, Geophys. Monogr. 99
Forbes, T. G., & Priest, E. R. 1995, ApJ, 446, 377
Gallagher, P. T., Dennis, B. R., Krucker, S., Schwartz, R. A., & Tolbert, A. K. 2002, Sol. Phys., 210, 341
Handy, B. N., et al. 1999, Sol. Phys., 187, 229
Klimchuk, J. A. 2001, Geophys. Monogr., 125, 143
Kohl, J. L., et al. 1995, Sol. Phys., 162, 313
Krall, J., Chen, J., Duffin, R. T., Howard, R. A., & Thompson, B. J. 2001, ApJ, 562, 1045
Krall, J., Chen, J., & Santoro, R. 2000, ApJ, 539, 964
Moon, Y.-J., Choe, G. S., Wang, H., Park, Y. D., Gopalswamy, N., Yang, G., & Yashiro, S. 2002, ApJ, 581, 694
Song, P., Singer, H. J., & Siscoe, G. L., eds. 2001, Geophys. Monogr. 125
St. Cyr, O. C., Burkepile, J. T., Hundhausen, A. J., & Lecinski, A. R. 1999, J. Geophys. Res., 104, 12,493
Wang, T. J., Solanki, S. K., Innes, D. E., & Curdt, W. 2002, in IAU Colloq. 188, Magnetic Coupling in the Solar Atmosphere (ESA SP-505; Noordwijk: ESA), 607
Zhang, J., Dere, K. P., Howard, R. A., Kundu, M. R., & White, S. 2001, ApJ, 559, 452